

accuracy derived from the experiment was: DD (5%) – 83.4% and 68% pixels passing, DTA (3mm) – 99.0% and 96.7%, gamma parameter (for DD (3%), DTA (3mm)) – 90% and 75.5% respectively for AAA and PBC algorithms. The comparison between studied parameters DD, DTA and γ for both algorithms implicated AAA as an appropriate approach in radiotherapy treatment planning.

Keywords: Radiotherapy planning algorithms, radiology, medical physics.

References:

- [1] – Gagné I M, Zavgorodni S, *Evaluation of the analytical anisotropic algorithm in an extreme water-lung interface phantom using Monte Carlo dose calculations*, Journal Of Applied Clinical Medical Physics, Vol. 7, 2007.
- [2] – International Commission on Radiation Units and Measurements (ICRU). *Determination of absorbed dose in a patient irradiated by beams of X or gamma rays in radiotherapy procedures*. ICRU Report 24, Washington (DC): ICRU, 1976.
- [3] – Van Escha A, Namur E, Tillikainen L, Pyykkonen J, Tenhunen M, Helminen H, Siljamäki S, Alakuijala J, Pajusco M, Iori M, Huyskens D P, *Testing of the analytical anisotropic algorithm for photon dose calculation*, American Association of Physicists in Medicine (AAPM), 2006.

182

Nuclear fragmentation in protontherapy

P. Rebello Teles¹, M. Hussein²

¹ Centro Brasileiro de Pesquisas Físicas, Rio de Janeiro, Brazil

² Instituto de Física, Universidade de São Paulo, São Paulo, Brazil

The effect of nuclear fragmentation in the passage of 180MeV protons through the human body tissue is discussed. Prostate cancer protontherapy with these intermediate-energy protons is discussed in light of model calculation.

Keywords: Nuclear fragmentation, protontherapy, prostate cancer

References:

- [1] G. Kraft, Tumor therapy with heavy charged particles, Progress in Particle and Nuclear Physics, 2000
- [2] A.J. Kreiner and A.A. Burlon, Novel Applications of Particle Accelerators to Radiotherapy, Heavy Ion Physics 16, 243 (2002)
- [3] B.V. Carlson, R.C. Mastroleo and M.S. Hussein, Phys. Rev. C46, R3 (1992);
- [4] B.V. Carlson, Phys. Rev. C51, 25 (1995)
- [5] A.S. Goldhaber, Phys. Lett. B 53, 306 (1974)

183

Internalization of iron nanoparticles by macrophages for the improvement of glioma treatment

S. Reymond^{1,2,3,4}, P. Gimenez^{1,2,3,4,9}, R. Serduc^{1,3}, J. Arnaud⁵, J.-P. Kleman⁶, V. Djonov⁷, W. Graber⁷, J.A. Laissue⁷, J.-K. Kim⁸, S.-J. Seo⁸, J.-L. Ravanat^{4,9,10}, H. Elleaume^{1,2,3,4}

¹ INSERM, U836, Grenoble, France;

² Université Joseph Fourier, Grenoble Institut des Neurosciences, UMR-S836, Grenoble, France;

³ European Synchrotron Radiation Facility, Grenoble, France;

⁴ LabEx PRIMES Lyon, France;

⁵ CHU Grenoble, France;

⁶ IBS Grenoble, France;

⁷ University of Berne, Bern, Switzerland;

⁸ Catholic University of Daegu, Daegu City, Korea;

⁹ INAC/SCIB LAN CEA-Grenoble, France;

¹⁰ Université de Grenoble, France

Rationale: An alternative approach for the improvement of radiotherapy consists in increasing differentially the radiation dose between tumors and healthy tissues using nanoparticles (NPs) that have been beforehand internalized into the tumor. These high-Z NPs can be photo-activated by monochromatic synchrotron X-rays, leading to a local dose enhancement delivered to the neighboring tumor cells[1]. This

enhancement is due to secondary and Auger electrons expelled from the NPs by the radiations. In order to carry the NPs into the tumor center, macrophages are currently under study for their phagocytosis and diapedesis abilities[2] (*cf.* Figure adapted from [3] and [4]). In this study we characterized J774A.1 macrophages' internalization kinetics and subcellular distribution of iron NPs and compared them to the internalization abilities of the F98 glioblastoma cell line.

Materials and Methods: Three aspects of internalization were examined: first, the *location of internalized NPs* in J774A.1 macrophages and F98 glioblastoma cells following a 24h incubation with iron NPs (0.3 mg/mL in the cell culture medium) was determined by optical microscopy after cell slicing. Subsequently, the *iron intake* after a 24h incubation with NPs (0.3 mg/mL and 0.06 mg/mL in the cell culture medium) was characterized for the two types of cells using ICP-MS. Finally, the *internalization dynamics* were studied by live phase-contrast microscopy imaging for 11 hours and by absorbance measurements for 24 hours using a plate reader.

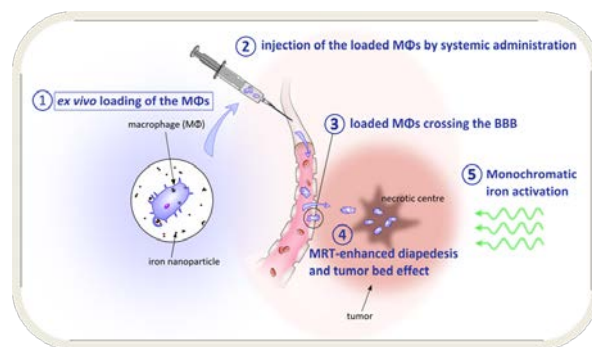
Results: F98 tumor cells and J774A.1 macrophages are both able to endocytose NPs: we measured $\sim 61 \pm 10$ pg of internalized iron per macrophage compared with $\sim 33 \pm 5$ pg per F98 cell (initial iron concentration: 0.3 mg/mL in culture medium). F98 internalizing NPs for 10 hours showed stress signs during the first minutes after the NPs injection, but behaved like F98 control cells during the rest of the experiment. Finally, we determined that the internalization kinetics for J774A.1 had a typical saturation time of one hour.

Conclusion: Macrophages seem to be promising vectors for NPs, being able to endocytose and retain in their cytoplasm larger quantities of NPs than tumor cells. Our following studies will attempt to shed light on their other potential abilities as "Trojan Horses".

Keywords: radiotherapy; nanoparticles; cell-carriers

References:

- [1] F. Taupin *et al.*, Phys Med Biol 60 (2015).
- [2] J. Choi *et al.*, Biomaterials 33 (2012).
- [3] R. Weissleder *et al.*, Nature Materials 13 (2014).
- [4] M.R. Choi *et al.*, Nano Letters 7 (2007).



184

First clinical application of a prompt gamma based *in vivo* proton range verification using a knife-edge slit camera

C. Richter¹⁻⁴, G. Pausch¹⁻³, S. Barczyk^{1,2}, M. Priegnitz³, I. Keitz¹, J. Thiele², J. Smeets⁵, F. Vander Stappen⁵, L. Bombelli⁶, C. Fiorini⁷, L. Hotolius⁵, I. Perali⁷, D. Prieels⁵, W. Enghardt¹⁻⁴, M. Baumann¹⁻⁴

¹ OncoRay - National Center for Radiation Research in Oncology, Faculty of Medicine and University Hospital Carl Gustav Carus, Technische Universität Dresden, Helmholtz-Zentrum Dresden - Rossendorf, Dresden, Germany

² Department of Radiation Oncology, University Hospital Carl Gustav Carus, Technische Universität Dresden, Dresden, Germany

³ Helmholtz-Zentrum Dresden - Rossendorf, Dresden, Germany

⁴ German Cancer Consortium (DKTK), Dresden, Germany and German Cancer Research Center (DKFZ), Heidelberg, Germany

⁵ Ion Beam Applications SA, Louvain-la-Neuve, Belgium

⁶ XGLab S.R.L., Milano, Italy

⁷ Politecnico di Milano, Dipartimento di Elettronica, Informazione e Bioingegneria, Milano, Italy

Purpose: To improve precision of particle therapy, in vivo range verification is highly desirable. Methods based on prompt gamma rays emitted during treatment seem promising but have not yet been applied clinically. Here we report on the worldwide first clinical application of prompt gamma imaging (PGI) based range verification.

Material / Methods: A prototype of a knife-edge shaped slit camera [1,2] was used to measure the prompt gamma ray depth distribution during a proton treatment of a head and neck tumor for seven consecutive fractions and one of three fields. The treatment was delivered with passively double scattered proton therapy (DS), although the slit camera was originally developed for pencil beam scanning. Before clinical application, the feasibility of the DS applicability was shown in a separate work [3], e.g. by introducing subtraction of the neutron-induced background. Inter-fractional variations of the prompt gamma profile were evaluated for the time integrated prompt gamma profile (sum profile) as well as for prompt gamma profiles corresponding to different steps of the modulator wheel (iso-energy layer resolved profile). For three fractions in-room control CTs were acquired and evaluated for dose relevant changes.

Results: The measurement of PGI profiles during proton treatment was successful. Based on the PGI information of the sum profiles, inter-fractional global range variations, determined with automated shift detection, were in the range of ± 2 mm for all evaluated fractions. This is within the uncertainty of the PGI system, as already the position accuracy of the PGI slit camera was determined with 1.1 mm (2σ). The detected range variations are in agreement with the control CT evaluation showing negligible range variations of about 1.5 mm. Also the evaluation of the iso-energy layer resolved prompt gamma profiles was in consistence with the analysis of the sum profiles and provided additional information.

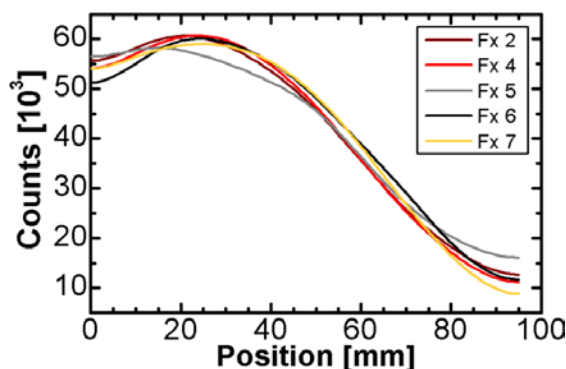


Figure 1: Detected PGI sum profiles for 5 fractions (Fx) after application of a Gaussian filter (FWHM=20 mm). The region between 20k-50k counts was used for automated shift detection. Please note that for two fractions no data were available - one was used for a background measurement with closed slit (Fx 3), and for another one (Fx 1) a deficient background subtraction disturbed the sum profile.

Conclusions: For the first time, range verification based on prompt gamma imaging was applied for a clinical proton treatment. Further plans include the continuation of the clinical study to perform systematic evaluations based on an appropriate patient number. With the translation from basic physics experiments into clinical operation, the authors are confident that a prompt gamma ray based technology is capable of range verification and can be used in the near future for online quality assurance as well as in midterm for potential margin reduction.

Keywords: prompt gamma imaging; range verification; slit camera

References:

- [1] Smeets, Roellinghoff, Prieels, Stichelbaut, Benilov, Busca, Fiorini, Peloso, Basilavecchia, Frizzi, Dehaes, Dubus: Prompt gamma imaging with a slit camera for real-time range control in proton therapy. *Phys. Med. Biol.*, 2012, 57, 3371-3405
- [2] Perali, Celani, Bombelli, Fiorini, Camera, Clementel, Henrotin, Janssens, Prieels, Roellinghoff, Smeets, Stichelbaut, Vander Stappen: Prompt gamma imaging of proton pencil beams at clinical dose rate. *Phys. Med. Biol.*, 2014, 59, 5849-5871
- [3] Priegnitz, Barczyk, Keitz, Mein, Vander Stappen, Janssens, Hotoiu, Smeets, Fiedler, Prieels, Enghardt, Pausch, Richter: Prompt gamma imaging of passively shaped proton fields with a knife-edge slit camera. Abstract submitted for ICTR-PHE 2016

185

Clinical applicability of the Compton camera for Prompt γ -ray Imaging during proton therapy

H. Rohling¹, M. Priegnitz¹, S. Schoene¹, A. Schumann¹, W. Enghardt^{2,3,4,5}, C. Golnik², F. Hueso-González³, T. Kormoll², G. Pausch², J. Petzoldt², K. Römer¹, F. Fiedler¹

¹Helmholtz-Zentrum Dresden - Rossendorf, Institute of Radiation Physics, Bautzner Landstr. 400, 01328 Dresden, Germany

²OncoRay - National Center for Radiation Research in Oncology, Faculty of Medicine and University Hospital Carl Gustav Carus, Technische Universität Dresden, Helmholtz-Zentrum Dresden - Rossendorf, Fetscherstr. 74, PF 41, 01307 Dresden, Germany

³Helmholtz-Zentrum Dresden - Rossendorf, Institute of Radiooncology, Bautzner Landstr. 400, 01328 Dresden, Germany

⁴Department of Radiation Oncology, Faculty of Medicine and University Hospital Carl Gustav Carus, Technische Universität Dresden, Fetscherstr. 74, 01307 Dresden, Germany

⁵German Cancer Consortium (DKTK), Dresden, Germany

Purpose: In order to guarantee the best outcome of a therapeutic irradiation with protons and other light ions a non-invasive in-vivo range verification is desired. One approach in this field is Prompt γ -ray Imaging (PGI). A possible detection system for the prompt γ -rays is the Compton camera. Several groups have been working on the construction of Compton camera prototypes [1-5]. Up to now, Compton cameras have not been used in clinical practice for the monitoring of particle therapy. By means of Geant4 simulations, we performed an end-to-end test to evaluate the clinical applicability of a Compton camera detection system and to determine the requirements regarding hardware and image reconstruction.

Materials/methods: First, a treatment plan for a therapeutic proton irradiation for the head-neck region was prepared using XiO (Electa AB, Sweden). Based on this treatment plan, the γ -ray emissions from the patient's tissue were simulated with Geant4. As a next step, the detector response was modelled, also with Geant4, for two large Compton cameras arranged around the patient in an angle of 90 degrees. Large-area detectors were already recommended [6]. Each camera was built up from a scatter layer (CZT) of dimension $10 \times 10 \times 0.5$ cm³ and an absorber layer (LSO) of size $20 \times 20 \times 2$ cm³. In practice, these cameras would be replaced by several smaller camera modules. For the simulation of the detector response a total number of previously simulated γ -ray emissions were used as input corresponding to an applied dose of 1 Gy, i.e. a common dose of one field of one treatment session. After extracting the resulting coincident events, the image was reconstructed using a 3D MLEM algorithm [7]. The impact of the number of events, filters, as well as background on the image quality was also studied.

Results: Figure 1 shows the images for the planned dose, the distribution of the γ -ray emissions and the reconstructed image obtained with 128 iterations of the MLEM algorithm. For the considered number of events and the chosen voxels